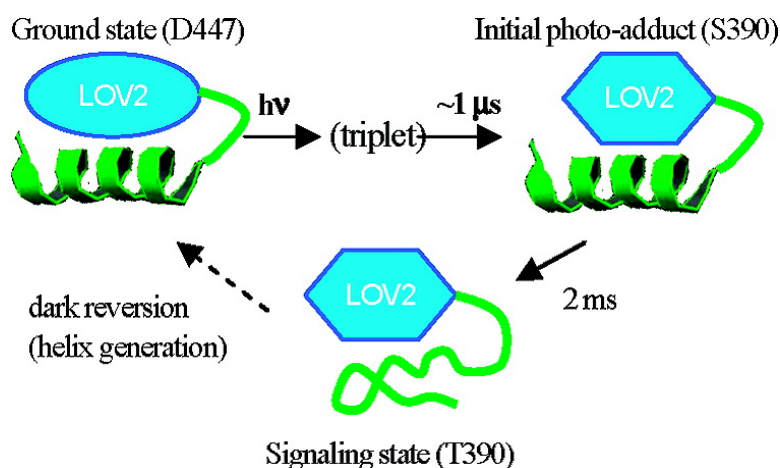


## Conformational Dynamics of Phototropin 2 LOV2 Domain with the Linker upon Photoexcitation

Takeshi Eitoku, Yusuke Nakasone, Daisuke Matsuoka, Satoru Tokutomi, and Masahide Terazima

*J. Am. Chem. Soc.*, **2005**, 127 (38), 13238-13244 • DOI: 10.1021/ja052523i • Publication Date (Web): 02 September 2005

Downloaded from <http://pubs.acs.org> on March 25, 2009



### More About This Article

Additional resources and features associated with this article are available within the HTML version:

- Supporting Information
- Links to the 12 articles that cite this article, as of the time of this article download
- Access to high resolution figures
- Links to articles and content related to this article
- Copyright permission to reproduce figures and/or text from this article

[View the Full Text HTML](#)

## Conformational Dynamics of Phototropin 2 LOV2 Domain with the Linker upon Photoexcitation

Takeshi Eitoku, Yusuke Nakasone, Daisuke Matsuoka,<sup>†</sup> Satoru Tokutomi,<sup>†</sup> and Masahide Terazima\*

Contribution from the Department of Chemistry, Graduate School of Science, Kyoto University, Kyoto, 606-8502, Japan, and Research Institute for Advanced Science and Technology, Osaka Prefecture University, Sakai, Osaka 599-8570, Japan

Received April 19, 2005; E-mail: mterazima@kuchem.kyoto-u.ac.jp

**Abstract:** Conformational dynamics of LOV2 domain of phototropin, a plant blue light photoreceptor, is studied by the pulsed laser induced transient grating (TG) technique. The TG signal of LOV2 without the linker part to the kinase domain exhibits the thermal grating signal due to the heat releasing from the excited state and a weak population grating by the adduct formation. The diffusion coefficients of the adduct product after forming the chemical bond between the chromophore and Cys residue are found to be slightly smaller than that of the reactant, which implies that the core shrinks slightly on the adduct formation. After that change, no significant conformational change was observed. On the other hand, the signal of LOV2 with the linker part to the kinase domain clearly shows very different diffusion coefficients between the original and the adduct species. The large difference indicates significant global conformational change of the protein moiety upon the adduct formation. More interestingly, the diffusion coefficient is found to be time-dependent in the observation time range. The dynamics representing the global conformational change is a clear indication of a spectral silent intermediate between the excited triplet state and the signaling product. From the temporal profile analysis of the signal, the rate of the conformational change is determined to be 2 ms.

### 1. Introduction

Phototropins (Phot1 and Phot2) are blue light receptors in higher plants for regulating phototropism, chloroplast relocations, and stomatal opening. Since all these are major regulation mechanisms to fine-tune the photosynthetic activities, phototropins are attracting much attention. Both proteins Phot1 and Phot2 are homologous flavoproteins and contain two light oxygen voltage sensing (LOV) domains (LOV1 and LOV2), a typical serine/threonine kinase at the C terminus, and one linker region connecting the LOV2 and the kinase domains acting as light-regulated protein kinase.<sup>1</sup> Both LOV domains bind a flavin mononucleotide (FMN) as chromophore.<sup>2,3</sup> The mechanism and the kinetics of the reaction have been attracting much attention recently.<sup>4</sup> The reaction kinetics has mainly been studied by monitoring the absorption change of the chromophore.<sup>5–8</sup> Upon

blue light illumination, the ground-state LOV2 possessing the absorption maximum at 447 nm (D447) is converted to a species with a broad absorption spectrum.<sup>9</sup> This change is attributed to the creation of the excited triplet state through the intersystem crossing from the photoexcited singlet state. This broad spectrum changes to a blue-shifted absorption spectrum peaked at 390 nm (S390) with a lifetime of 4  $\mu$ s (for Phot1 LOV2 of *Avena*).<sup>9</sup> This species is assigned to the FMN–cysteinyl adduct, in which the sulfur covalently binds to the C(4a) carbon of the isoalloxazine ring of FMN. This adduct is stable for tens of seconds before returning back to the ground state.<sup>10</sup> The assignment of this product has been confirmed by NMR,<sup>11</sup> X-ray crystallography,<sup>12–14</sup> and FT-IR.<sup>15</sup> It is believed that this state is the signaling state. Therefore, as long as the reaction kinetics is monitored by the UV–vis spectroscopy, the signaling state is formed with a lifetime of 4  $\mu$ s, and no significant dynamics

<sup>†</sup> Present address: Department of Biological Science, Graduate School of Science, Osaka Prefecture University, Sakai, Osaka, 599-8531, Japan.  
(1) Huala, E.; Oeller, P. W.; Liscum, E.; Han, I.; Larsen, E.; Briggs, W. R. *Science* **1997**, *278*, 2120.  
(2) Christie, J. M.; Reymond, P.; Powell, G. K.; Bernasconi, P.; Raibekas, A. A.; Liscum, E.; Briggs, W. R. *Science* **1998**, *282*, 1698.  
(3) Christie, J. M.; Salomon, M.; Nozue, K.; Wada, M.; Briggs, W. R. *Proc. Natl. Acad. Sci. U.S.A.* **1999**, *96*, 8779.  
(4) Salomon, M.; Christie, J. M.; Knieb, E.; Lempert, U.; Briggs, W. R. *Biochemistry* **2000**, *39*, 9401.  
(5) Schleicher, E.; Kowalczyk, R. M.; Kay, C. W. M.; Hegemann, P.; Bacher, A.; Fischer, M.; Bittl, R.; Richter, G.; Weber, S. *J. Am. Chem. Soc.* **2004**, *126*, 11067.  
(6) Kottke, T.; Heberle, J.; Hehn, D.; Dick, B.; Hegemann, P. *Biophys. J.* **2003**, *84*, 1192.  
(7) Schüttrigkeit, T. A.; Kompa, C. K.; Salomon, M.; Rüdiger, W.; Michel-Beyerle, M. E. *Chem. Phys.* **2003**, *294*, 501.

(8) Kennis, J. T. M.; Crosson, S.; Gauden, M.; van Stokkum, I. H. M.; Moffat, K.; van Grondelle, R. *Biochemistry* **2003**, *42*, 3385.  
(9) Swartz, T. E.; Corchnoy, S. B.; Christie, J. M.; Lewis, J. W.; Szundi, I.; Briggs, W. R.; Bogomolni, R. A. *J. Biol. Chem.* **2001**, *276*, 36493.  
(10) Kasahara, M.; Swartz, T. E.; Olney, M. A.; Onodera, A.; Mochizuki, N.; Fukuzawa, H.; Asamizu, E.; Tabata, S.; Kanegae, H.; Takano, M.; Christie, J. M.; Nagatani, A.; Briggs, W. R. *Plant Physiol.* **2002**, *129*, 762.  
(11) Salomon, M.; Eisenreich, W.; Dürr, H.; Schleicher, E.; Knieb, E.; Massey, V.; Rüdiger, W.; Müller, F.; Bacher, A.; Richter, G. *Proc. Natl. Acad. Sci. U.S.A.* **2001**, *98*, 12357.  
(12) Fedorov, R.; Schlichting, I.; Hartmann, E.; Domratcheva, T.; Fuhrmann, M.; Hegemann, P. *Biophys. J.* **2003**, *84*, 2474.  
(13) Crosson, S.; Moffat, K. *Proc. Natl. Acad. Sci. U.S.A.* **2001**, *98*, 2995.  
(14) Crosson, S.; Moffat, K. *Plant Cell* **2002**, *14*, 1067.  
(15) Swartz, T. E.; Wenzel, P. J.; Corchnoy, S. B.; Briggs, W. R.; Bogomolni, R. A. *Biochemistry* **2002**, *41*, 7183.



**Figure 1.** Schematic illustration of the LOV2 sample and LOV2-linker sample we used.

has been reported after this process. The fast rate may suggest that the global structural change is not required for the signaling. This idea seems to be consistent with the X-ray crystallographic data showing that the protein structure under light illumination is not so different from that in the dark except for the chemical bonding of the chromophore with cysteine for *Chlamydomonas* Phot LOV1<sup>12</sup> and *Adiantum* phytochrome3 LOV2.<sup>13</sup> However, other spectroscopic data suggested more pronounced structural rearrangement.<sup>16–18</sup> If conformational change occurs, can such global motion complete within 4  $\mu$ s? There is no evidence for or against this suggestion thus far. In this study, we investigate the conformational dynamics of the *Arabidopsis* Phot2 LOV2 in time domain from a new viewpoint.

Although optical absorption change in time domain has been used frequently for studying reaction dynamics of proteins, we should always be careful with the fact that the whole protein size is very large compared with that of the chromophore. Since the absorption spectrum of the chromophore is sensitive to only conformational change close to the chromophore, the dynamics that can be monitored by the optical transition could not be all of them. The structural change far from the chromophore as well as the dynamics of the intermolecular interaction (spectral silent process) are very important for biological function, and hence, these dynamics should be detected under physiological conditions. In this respect, one of the transport properties, the translational diffusion coefficient ( $D$ ), is a good physical property reflecting the conformational change and the intermolecular interaction.<sup>19</sup> A difficulty for utilizing the diffusion process as the dynamics monitoring method is the rather slow response of the traditional diffusion detection techniques (e.g., several hours for using the Taylor dispersion method and several minutes for the light scattering technique). However, the pulsed laser induced transient grating (TG) method recently enabled us to open the spectral silent dynamics measurement by the diffusion probing.<sup>20–25</sup> In this article, we report the protein dynamics of Phot2 LOV2 domain (18 kDa: LOV2 sample) and Phot2 LOV2 with the linker (25 kDa: LOV2-linker sample) (Figure 1) by monitoring the dynamics of  $D$ . We found the first evidence for the large conformational change with a lifetime of 2 ms; that is, there are “dark” intermediate species during the photocycle of Phot2 that have not been detected thus far. The new intermediate species should possess a similar conformation around the chromophore, because it is spectrally silent, but the intermolecular interaction is dramatically different. The

dynamics is observed for the LOV2-linker sample but not for the LOV2 without the linker, showing that the conformation of the linker part is considerably altered by the photoreaction. We suggest that the intramolecular hydrogen bonding of the  $\alpha$ -helix in the linker part is broken during this process. This process should significantly alter the interdomain interaction between the LOV2 domain and the kinase domain.

## 2. Experimental Section

**2.1. Measurement.** The experimental setup was similar to that reported previously.<sup>20–24</sup> Briefly, a laser pulse from a dye laser (Lumomics, HyperDye 300; wavelength = 465 nm) pumped by an excimer laser (Lambda Physik, XeCl operation; 308 nm) was used as an excitation beam and a diode laser (835 nm) was used as a probe beam. The excitation beam was split into two by a beam splitter and crossed inside a sample cell. The sample is photoexcited by the created interference pattern to induce the refractive index modulation in the sample. A part of the probe beam was diffracted by the modulation (TG signal). The signal was isolated from the excitation laser beam with a glass filter and a pinhole, detected by a photomultiplier tube (Hamamatsu R1477), and recorded by a digital oscilloscope. The spacing of the fringe was measured by the decay rate constant of the thermal grating signal from a calorimetric standard sample, which releases all the photon energy of the excitation as the thermal energy within a time response of our system. All measurements were carried out at room temperature.

**2.2. Preparation of Recombinant LOV Polypeptides.** *Arabidopsis* Phot2 LOV2 (363D-500Q) and LOV2-linker polypeptides (363D-575H) (Figure 1) were prepared by overexpression systems with *Escherichia coli* as described in ref 26. The LOV2 polypeptides included additional extensions of some amino acid residues at both the N- and the C-terminal ends of the LOV core (388E-492G). In addition, both polypeptides have a linker sequence (Gly-Ser-Pro-Glu-Phe) at their N-termini. GST-tag-cleaved polypeptides were purified by a gel chromatography with Sephacryl S-100 HR (Pharmacia) and a buffer solution containing 100 mM NaCl, 25 mM Tris-HCl, and 1 mM Na<sub>2</sub>EDTA (pH 7.8). The eluted polypeptide solutions showed single bands upon Coomassie Brilliant Blue staining after SDS polyacrylamide gel electrophoresis. The molecular mass of either recombinant polypeptide and the purity of the sample were also examined by time-of-flight mass spectrometry with an AXIMA-QIT instrument (Shimadzu). The purified LOV polypeptides in the buffer described above were concentrated by ultrafiltration and then used for TG measurements. The concentration for most experiments was about 1–3 mg/mL. For examining the concentration dependence, a concentration range of 0.4–1 mg/mL was used.

## 3. Principle and Theoretical

In the TG experiment, a photoinduced reaction is initiated by the spatially modulated light intensity that is produced by the interference of two excitation light waves.<sup>20–24</sup> The sinusoidal modulations of the concentrations of the reactant and the product lead to the sinusoidal modulation in the refractive index ( $\delta n$ ). This modulation can be monitored by the diffraction efficiency of a probe beam (TG signal). In this experiment, the refractive index change mainly comes from the thermal energy releasing (thermal grating;  $\delta n_{th}(t)$ ) and creating (or depleting) chemical species by the photoreaction (species grating). The species grating consists of two contributions: population grating and the volume grating. The volume grating term comes from

(16) Harper, S. M.; Neil, L. C.; Day, I. J.; Hore, P. J.; Gardner, K. H. *J. Am. Chem. Soc.* **2004**, *126*, 3390.

(17) Harper, S. M.; Neil, L. C.; Gardner, K. H. *Science* **2003**, *301*, 1541.

(18) Corchnoy, S. B.; Swartz, T. E.; Lewis, J. W.; Szundi, I.; Briggs, W. R.; Bogomolni, R. A. *J. Biol. Chem.* **2003**, *278*, 724.

(19) Choi, J.; Terazima, M. *J. Phys. Chem. B* **2002**, *106*, 6587.

(20) Terazima, M.; Hirota, N. *J. Chem. Phys.* **1993**, *98*, 6257.

(21) Terazima, M.; Okamoto, K.; Hirota, N. *J. Chem. Phys.* **1995**, *102*, 2506.

(22) Terazima, M. *Adv. Photochem.* **1998**, *24*, 255.

(23) Terazima, M. *Acc. Chem. Res.* **2000**, *33*, 687.

(24) Nada, T.; Terazima, M. *Biophys. J.* **2003**, *85*, 1876.

(25) Nishida, S.; Nada, T.; Terazima, M. *Biophys. J.* **2004**, *87*, 2663.

(26) Nakasako, M.; Iwata, T.; Matsuoka, D.; Tokutomi, S. *Biochemistry* **2004**, *43*, 14881.

the density change caused by the molecular volume change by the reaction. The population grating is caused by the refractive index change associated with the absorption change of the chemical species.<sup>22,23</sup> This refractive index is related to the absorption spectrum through the Lorenz–Lorentz relationship so that the refractive index change is observable in a wavelength region much wider than that of the absorption change.<sup>22,23</sup> The species grating signal intensity is given by the difference of the refractive index changes due to the reactant ( $\delta n_r$ ) and product ( $\delta n_p$ ):

$$I_{\text{TG}}(t) = \alpha[\delta n_{\text{th}}(t) + \delta n_r(t) - \delta n_p(t)]^2 \quad (1)$$

where  $\alpha$  is a constant. The term of  $\delta n_p$  is negative, because the depletion of the reactant causes a 180°-shifted phase of the spatial concentration modulation of the reactant from that of the product. The species grating signal intensity becomes weaker as the spatial modulations of the refractive index become uniform, which is accomplished by the translational diffusion. Temporal development and the spatial distribution of concentration of chemical species ( $C(x,t)$ ) is calculated by solving a diffusion equation:

$$\frac{\partial C(x,t)}{\partial t} = D \frac{\partial^2 C(x,t)}{\partial x^2} \quad (2)$$

where  $x$  is a direction along the grating wave vector and  $D$  is the diffusion coefficient of the chemical species. Solving this diffusion equation by using the Fourier transform method under an assumption of constant  $D$ , we may find that the  $q$ -Fourier component of the concentration decays with a rate constant of  $Dq^2$ . Hence, the time development of the TG signal can be expressed by a biexponential function.<sup>20–24</sup>

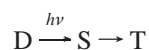
$$I_{\text{TG}}(t) = \alpha[\delta n_{\text{th}}(t) + \delta n_r \exp(-D_r q^2 t) - \delta n_p \exp(-D_p q^2 t)]^2 \quad (3)$$

where  $D_r$  and  $D_p$  are diffusion coefficients of the reactant and the product, respectively. Furthermore,  $\delta n_r$  ( $>0$ ) and  $\delta n_p$  ( $>0$ ) are, respectively, the initial refractive index changes due to the presence of the reactant and the product. Similarly, the thermal grating signal decays by a function of

$$\delta n_{\text{th}}(t) = \delta n_{\text{th}} \exp(-D_{\text{th}} q^2 t)$$

where  $D_{\text{th}}$  is the thermal diffusivity of the solution.

When  $D$  is time-dependent, the observed TG signal should be significantly different from that predicted by eq 3. For analyzing the observed TG signal in this study, the following model was used.



D, S, and T represent the ground state of LOV2 (D447), the initial product (after formation of the adduct S390), and final product, which possesses the same absorption spectrum as S390, respectively. If we assume that the conformational transition between two states occurs with a rate constant  $k$ , the time dependence of the concentrations of S390 ([S]) and the final

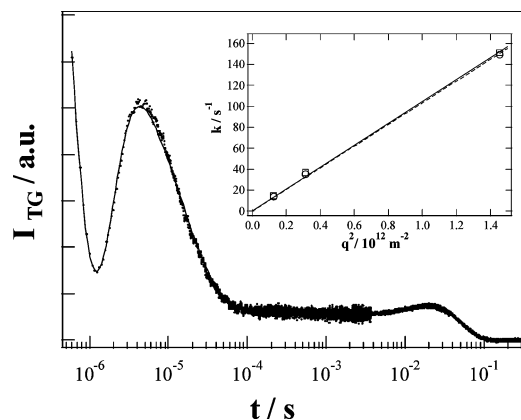


**Figure 2.** Observed TG signal (dotted line) of LOV2 without the linker sample at  $q^2 = 3.1 \times 10^{11} \text{ m}^{-2}$ . The best fitted curve based on eq 6 is shown by the solid line. (Inset) The  $q^2$  plot of the rise and decay rate constants of the diffusion signal ( $\circ$ : reactant;  $\square$ : product). The solid and broken lines are the best fitted lines with  $k = Dq^2$ . The data and the lines are almost overlapped because of the very similar diffusion coefficients between  $D_p$  and  $D_r$ . The diffusion signal at around 10 ms is very weak compared with the thermal grating signal, which appears at a few microseconds.

product ([T]) are governed by diffusion equations of

$$\begin{aligned} \frac{\partial [S(x,t)]}{\partial t} &= D_S \frac{\partial^2 [S(x,t)]}{\partial x^2} - k[S(x,t)] \\ \frac{\partial [T(x,t)]}{\partial t} &= D_T \frac{\partial^2 [T(x,t)]}{\partial x^2} + k[S(x,t)] \end{aligned} \quad (4)$$

Solving these equations, we may find the time dependence of the refractive index as<sup>25</sup>

$$\begin{aligned} \delta n_p(t) &= \delta n_S \exp[-(D_S q^2 + k)t] + \\ &\quad \frac{\delta n_T k}{(D_T - D_S)q^2 - k} \{ \exp[-(D_S q^2 + k)t] - \exp(-D_T q^2 t) \} \\ \delta n_r(t) &= \delta n_D \exp(-D_D q^2 t) \end{aligned} \quad (5)$$

The temporal profile of the TG signal based on this model is calculated from eqs 1 and 5.

## 4. Results

**4.1. TG Signal of LOV2 Sample.** Figure 2 depicts the TG signal after the photoexcitation of the LOV2 sample (without the linker part). The signal rises quickly with the time response of our system ( $\sim 10$  ns). First, the signal decays within a few microseconds, rises, and then decays. After the decay in the microseconds time range, the signal intensity remains almost constant during two orders of time range, shows weak rise component, and finally decays to the baseline. This temporal profile can be reproduced well with a sum of four exponential functions.

$$I_{\text{TG}}(t) = \alpha[a_1 \exp(-k_1 t) + a_2 \exp(-k_2 t) + a_3 \exp(-k_3 t) + a_4 \exp(-k_4 t)]^2 \quad (6)$$

where  $k_1 > k_2 > k_3 > k_4$ . For the assignment of these components, we measured the signal under different grating wavenumbers ( $q^2$ ). It was found that the fastest decay rate constant ( $k_1$ ) is always  $(0.9 \mu\text{s})^{-1}$ , and this value does not depend

on  $q^2$ . The  $q^2$  independence indicates that this dynamics represents a chemical reaction rate. Since this rate is close to that reported for the D447  $\rightarrow$  S390 process of *Avena* ( $4 \mu\text{s}$ )<sup>-1</sup>,<sup>9</sup> we attribute the main contribution of this component to the population grating signal representing the absorption change associated with the adduct formation and small volume grating signal, which has been detected by the photoacoustic method.<sup>27,28</sup> In another sample, *Chlamydomonas* Phot LOV1, the kinetics of the adduct formation was reported to be biphasic with rates of ( $0.8 \mu\text{s}$ )<sup>-1</sup> and ( $4 \mu\text{s}$ )<sup>-1</sup>.<sup>29</sup> The slightly different lifetime of  $0.9 \mu\text{s}$  from the reported ones may be due to the different sample.

The other rate constants depend on  $q^2$ . This  $q^2$  dependence indicates that these dynamics represent the diffusion process. By comparing with the thermal grating signal from a calorimetric reference sample (bromocresol purple), which decays with a rate constant of  $D_{\text{th}}q^2$ , we found that  $k_2$  agrees with this constant. Hence, this is the thermal grating component created by the thermal energy due to the nonradiative transition from the excited state (i.e.,  $a_2 = \delta n_{\text{th}}$ , and  $k_2 = D_{\text{th}}q^2$ ).

The slower  $q^2$ -dependent rates,  $k_3$  and  $k_4$ , should represent the molecular diffusion process. This last rise–decay curve (diffusion signal) can be fitted by the last two exponential terms of eq 6 with  $a_3 > 0$ ,  $a_4 < 0$ , and  $|a_3| < |a_4|$ . The sign of the pre-exponential factor can be determined without any ambiguity by using the fact that the sign of the thermal grating signal is negative ( $\delta n_{\text{th}} < 0$ ). The diffusing species can be assigned from the sign of the pre-exponential factors. Comparing the fitting results of  $a_3 > 0$  and  $a_4 < 0$  with eq 3, we can easily attribute the  $a_3$  and  $a_4$  terms of eq 6 to the  $\delta n_{\text{p}}$  and  $\delta n_{\text{r}}$  terms of eq 3, respectively. Hence, the rate constants of  $k_3$  and  $k_4$  should correspond to  $D_{\text{p}}q^2$  and  $D_{\text{r}}q^2$ , respectively. On the basis of this finding and  $k_3 > k_4$ , we conclude that  $D_{\text{p}}$  is larger than  $D_{\text{r}}$ ; that is, the adduct product diffuses faster than the original species.

For determining  $D_{\text{p}}$  and  $D_{\text{r}}$ , the rate constants of the rise–decay curve ( $k_3$  and  $k_4$ ) should be determined by the curve fitting of the signal. However, using the four adjustable parameters ( $a_3$ ,  $a_4$ ,  $k_3$ ,  $k_4$ ) for the fitting, we found that there is rather large ambiguity for the fitting. We have to reduce the number of adjustable parameters for reliable fitting. Hence, we assume that the refractive index change due to the reactant ( $\delta n_{\text{r}}$ ) and the product ( $\delta n_{\text{p}}$ ), which reflect the molecular polarizabilities of the chemical species, is much larger than that of the thermal grating contribution ( $\delta n_{\text{th}}$ ). This assumption is reasonable and confirmed by the TG signal of the LOV2-linker sample as follows. Since the absorption spectra of the LOV2 and LOV2-linker sample are almost identical,  $\delta n_{\text{r}}$  and  $\delta n_{\text{p}}$  of LOV2 and LOV2-linker samples should be very similar. As described in the next section, we observe a very strong diffusion signal compared with the thermal grating signal for the LOV2-linker sample ( $\delta n_{\text{r}}/\delta n_{\text{th}} \approx 30$ ). If we use this value for the LOV2 sample, we can uniquely determine  $k_3$  and  $k_4$ . From the slopes of the plot of  $k_3$  and  $k_4$  against  $q^2$  (inset of Figure 2),  $D_{\text{p}}$  and  $D_{\text{r}}$  are determined to be  $10.5 \times 10^{-11}$  and  $10.3 \times 10^{-11}$  m<sup>2</sup>/s, respectively. (As long as we use  $\delta n_{\text{r}}/\delta n_{\text{th}} > 8$ , the determined  $D_{\text{p}}$  and  $D_{\text{r}}$  are rather insensitive (within  $\pm 5\%$ ) to the exact value of  $\delta n_{\text{r}}/\delta n_{\text{th}}$ .) It is interesting to note that, although  $D_{\text{p}}$  is certainly

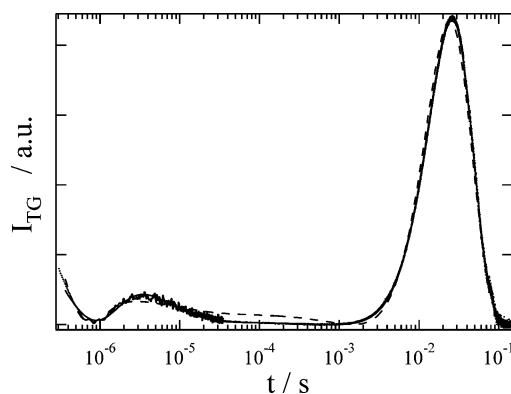


**Figure 3.** Observed TG signal (dotted line) of the LOV2 with the linker sample at  $q^2 = 5.6 \times 10^{11} \text{ m}^{-2}$ . The best fitted curve by the biexponential function based on eq 3 is shown by the dotted line. The best fitted curve by the time-dependent  $D$  is shown by the solid line, which is almost completely overlapped with the signal. Note the very strong diffusion signal at around 10 ms compared with the thermal grating signal, which appears at a few microseconds.

larger than  $D_{\text{r}}$ , the difference is very small. The small difference in  $D$  indicates that the conformational change by forming the adduct is small for the LOV2 sample.

**4.2. TG Signal of LOV2-Linker Sample.** Figure 3 depicts the TG signal of the LOV2-linker sample. The feature in a fast time region ( $0\text{--}100 \mu\text{s}$ ) is similar to that of LOV2 sample. The signal rises quickly and decays with a lifetime of  $0.8 \mu\text{s}$  and with  $D_{\text{th}}q^2$ . The initial decay should be attributed to the transformation from D447 to S390. The very similar lifetime of the S390 creation for the LOV2-linker sample to that for the LOV2 sample indicates that the linker part does not affect the kinetics of the adduct formation. This conclusion is reasonable, because the linker part is located apart from the chromophore.<sup>17</sup>

On the other hand, the species grating signal after the thermal grating signal is very different from that of the LOV2 sample. The signal reaches the baseline, and a strong rise–decay signal appears. Since the time range of this signal depends on the grating wavenumber, this signal is certainly originated by the molecular diffusion process (diffusion signal). The fact that the signal decays once to the baseline before the diffusion signal ( $\sim 0.4$  ms in Figure 3) and that  $\delta n_{\text{th}}$  is negative at this temperature clearly indicates that the rise component corresponds to the negative change of the refractive index ( $\delta n < 0$ ) and the subsequent decay component to the positive change. From the sign of these refractive index changes, we attribute the rise and decay component of the TG signal to the diffusion process of the reactant (ground state protein; (D447)) and the photoproduct, respectively (eq 3).

If  $D$  is time-independent,  $D$  can be determined from the rate constant of the rise and decay at various  $q^2$  values based on eq 6. However, we found that the profile cannot be fitted by the biexponential function (Figure 3). This fact indicates that the reaction cannot be a simple transformation from the ground state (D447) to the adduct product (S390). Although this fact does not necessarily mean that the diffusion coefficient is time-dependent, we found two more pieces of evidence showing that the signal should be analyzed by the time-dependent  $D$ . First, if the profile represents only the diffusion process, the time dependence should be expressed by a combination of terms of  $\exp(-Dq^2t)$  (e.g., eq 3). In this case, if the signal measured at various  $q^2$  is plotted against  $q^2t$ , the shape of the signals should

(27) Losi, A.; Kottke, T.; Hegemann, P. *Biophys. J.* **2004**, *86*, 1051.

(28) Losi, A.; Braslavsky, S. E. *Phys. Chem. Chem. Phys.* **2003**, *5*, 2739.

(29) Kottke, T.; Heberle, J.; Hehn, D.; Dick, B.; Hegemann, P. *Biophys. J.* **2003**, *84*, 1192.

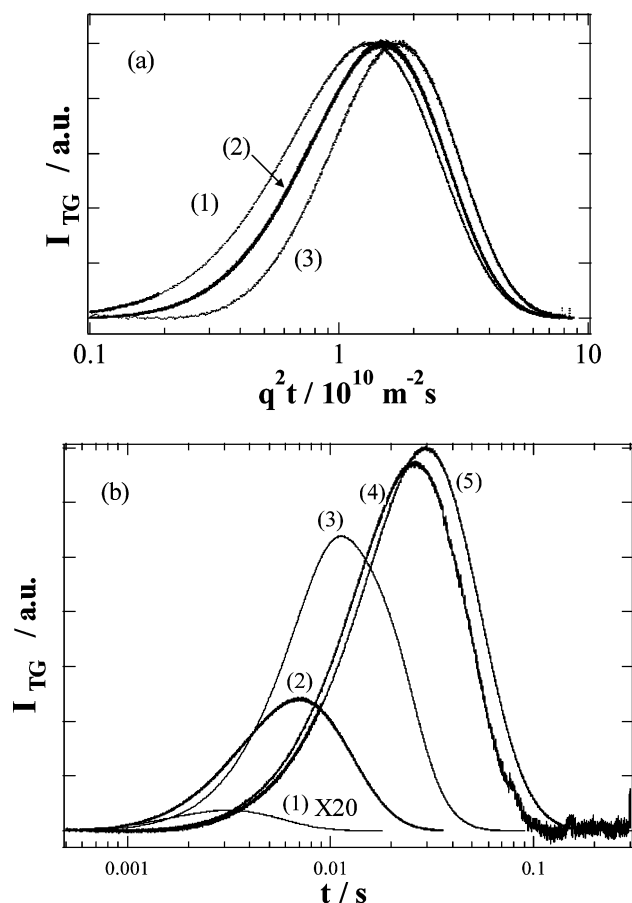


**Figure 4.** (a) TG signals of the LOV2 with the linker sample at various  $q^2$  plotted against  $q^2 t$ . The  $q^2$  values are (1)  $1.25 \times 10^{10}$ , (2)  $2.14 \times 10^{12}$ , and (3)  $9.09 \times 10^{12} \text{ m}^{-2}$ . (b) Signal intensity at various  $q^2$  normalized by the thermal grating signal intensity. The  $q^2$  values are (1)  $5.0 \times 10^{12}$ , (2)  $2.13 \times 10^{12}$ , (3)  $1.16 \times 10^{12}$ , (4)  $5.63 \times 10^{11}$ , and (5)  $5.60 \times 10^{11} \text{ m}^{-2}$ .

be identical. However, the signals are totally different depending on the  $q^2$  value (Figure 4a). Therefore, the failure of the biexponential function cannot be explained by simply adding more diffusion terms. Second, we found that the species grating signal intensity of the LOV2-linker sample depends on the observation time. If the conformational dynamics completes within a few microseconds as suggested by the flash photolysis technique, the species grating signal intensity should not depend on  $q^2$ . Contrary to this expectation, the TG signal in a fast time scale (with a large  $q^2$ ) is weak and the intensity increases with increasing observation time by decreasing  $q^2$  (Figure 4b). This observation time dependence of the signal intensity can be explained in terms of the time-dependent diffusion coefficient as follows. Considering a condition of  $\delta n_p \approx \delta n_r$  in eq 3, the signal intensity should be weak for  $D_p \approx D_r$ , because of the cancellation of the two terms in eq 3. With increasing difference between  $D_p$  and  $D_r$ , the apparent signal intensity becomes stronger. Since  $D$  of the reactant should be constant, the time dependence of the signal intensity should come from the time-dependent decrease of  $D_p$ . On the basis of these facts and considerations, we conclude that  $D$  is not constant in this time range but time-dependent.

In the long history of the diffusion study until now,  $D$  has always been considered to be a static character. However, recently, time-dependent  $D$  has been observed by using the TG method during the protein folding process.<sup>24,25</sup> The result

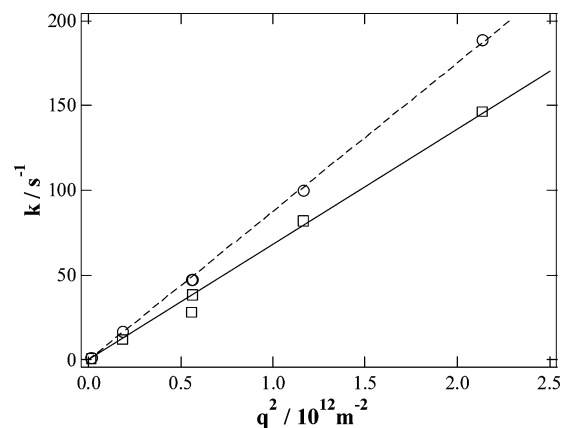


**Figure 5.** The  $q^2$ -plot of the rise and decay rate constants determined from the biexponential fitting of the TG signal of the LOV2 with the linker sample after 20 ms. Circles and squares represent the reactant and the product, respectively. The solid and broken lines are the best fitted lines with  $k = Dq^2$ .

presented here is the first report showing that  $D$  is changing during chemical reaction of the protein.

**4.3. Conformational Change of LOV2-Linker.** We have to analyze the species grating signal using a time-dependent diffusion model. However, before analyzing the TG data, it is instructive and important to determine  $D$  of the final product of the LOV2-linker sample first. After any conformational change completes,  $D$  should be time-independent. Therefore, the temporal profile of the TG signal after this time should be expressed by a biexponential function (eq 3). To roughly estimate this time, we used the  $q^2$  dependence of the signal intensity (Figure 4b). As explained in the previous section, the species grating intensity is a good indicator of the difference in  $D$ . The signal intensity does not change so much after 20 ms. Later we will find that this time is sufficiently longer than the lifetime of the  $D$  change (i.e., the dynamics of  $D$  has been completed at this time). On the basis of this fact, we first tried to fit the data by a biexponential function after 20 ms and found that the temporal profile after this time can actually be fitted well by a biexponential function. The rate constants of the rise ( $k_r$ ) and decay ( $k_d$ ) from the TG signal measured at various  $q^2$  are plotted against  $q^2$  in Figure 5. The figure clearly shows the linear relationship between the rate constants and  $q^2$  as expected from eq 3. The good fitting by the biexponential function and this linear relationship ensure that  $D$  does not depend on time after 20 ms. From the slope of the plots,  $D_p$  and  $D_r$  are determined to be  $(6.8 \pm 0.4) \times 10^{-11} \text{ m}^2/\text{s}$  and  $(8.8 \pm 0.4) \times 10^{-11} \text{ m}^2/\text{s}$ .

The large difference in  $D$  between the reactant and product is striking. According to the Stokes–Einstein relationship,  $D$  is given by<sup>30,31</sup>

$$D = k_B T / a \eta r \quad (7)$$

where  $k_B$ ,  $T$ ,  $\eta$ ,  $a$ , and  $r$  are Boltzmann constant, temperature, viscosity, a constant representing the boundary condition between the diffusing molecule and the solvent, and radius of the molecule, respectively. If the difference in  $D$  between the

(30) Cussler, E. L. *Diffusion, Mass Transfer in Fluid Systems*; Cambridge University Press: Cambridge, 1984.

(31) Tyrrell, H. J. V.; Harris, K. R. *Diffusion in Liquids: A Theoretical and Experimental Study*; Butterworths: London, 1984.

reactant and product is interpreted in terms of the difference in the molecular radius, the molecular volume of the product should be 2.2 times larger than that of the reactant. However, it is unrealistic to consider that the intrinsic molecular volume increases 2.2 times by the chemical reaction. Indeed, the small-angle X-ray scattering (SAXS) experiment indicates that the radius of gyration in the dark state (2.43 nm) increases slightly to 2.50 nm upon the light irradiation.<sup>26</sup> The increase of the radius (1.03 times) cannot explain the drastic change in  $D$  observed here.

One possible explanation for the large reduction of  $D$  is the dimerization of the LOV2-linker protein after the adduct reaction. To examine this possibility, we measured the TG signal at various concentrations. If the dimerization is the main cause of the large difference in  $D$ , this reaction rate should be slower at a lower concentration. However, we found that the time profile of the TG signal at different concentrations (2–0.4 mg/mL) is almost the same. Furthermore, the SAXS experiment showed that the Phot2 LOV2 domain exists in the monomeric form before photo illumination in a concentration range of 1–4 mg/mL and no light-dependent association was observed.<sup>26</sup> Hence, we exclude the dimerization reaction as the cause of the change in  $D$ .

This large decrease in  $D$ , instead, may be attributable to the increased intermolecular interactions between protein and water molecules as we have observed with cytochrome *c* (Cyt *c*) previously.<sup>24,25</sup> Cyt *c* is known to be mainly composed of  $\alpha$ -helices that are supported by intramolecular hydrogen bonding. Denaturation of Cyt *c* induces unfolding of the helices that accompanies rearrangement of hydrogen bonding from intramolecular to intermolecular between the protein and water molecules. This intermolecular interaction acts as a friction for the translational movement to reduce the diffusion coefficient by changing  $a$  in eq 7. The change makes  $D$  almost half that of the native Cyt *c*, which is comparable to the change of Phot2 LOV2-linker. The large decrease in  $D$ , hence, can be explained mostly with the increased intermolecular interactions, although the contribution of conformational changes that alter  $r$ , especially those in the interdomain interactions between the LOV2 core domain and the linker region, cannot be excluded completely.

It is particularly interesting to note that  $D_p$  is slightly smaller than  $D_r$  for the LOV2-linker sample, whereas  $D_p$  is larger than  $D_r$  for the LOV2 sample. The smaller  $D_r$  than  $D_p$  of the LOV2 sample, although the difference is small, indicates that the LOV2 domain itself becomes rather compact by the adduct formation. This structural change by the adduct formation is consistent with the volume change accompanying this process detected by the photoacoustic method.<sup>27,28</sup> The behavior is opposite for the linker sample. This difference should come from the conformation at the linker part. The SAXS experiment showed that the linker region forms a compact structure rather than a flexible loop conformation.<sup>26</sup> NMR study on oat Phot1 LOV2 revealed the presence of an  $\alpha$ -helix, named J-helix, in a part of the linker region. Its interaction with the LOV2 core changes on the photoreaction.<sup>17</sup> Furthermore, light-induced changes in the far-UV circular dichroism (CD) spectrum of oat Phot1 LOV2 showed a reversible loss of  $\alpha$ -helicity upon light irradiation.<sup>18</sup> In consideration of these results, the drastic reduction in  $D$  of the LOV2-linker protein on the photoreaction can be ascribed

**Table 1.** Diffusion Coefficients of the LOV2 and LOV2-Linker Samples ( $D/10^{-11}$  m<sup>2</sup>/s) and the Rate Constant ( $k/s^{-1}$ ) of the T390  $\rightarrow$  Product Process Determined by the Fitting of the TG Signal<sup>a</sup>

	$D$			$k/s^{-1}$
	D447	S390	T390	
LOV2	10.3	10.5	—	—
LOV2-linker	8.8	(8.8) <sup>b</sup>	6.8	500

<sup>a</sup> The error of  $D$  is  $\pm 0.4 \times 10^{-11}$  m<sup>2</sup>/s. <sup>b</sup> Since  $D$  does not change so much by the photoadduct formation as shown from the results of the LOV2 sample,  $D$  of S390 of the LOV2-linker sample is assumed to be the same as that of D447.

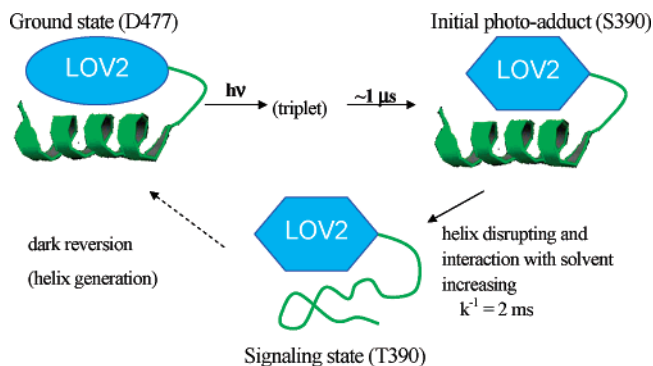


**Figure 6.** Schematic showing the reaction process of LOV2-linker sample.

mainly to the reorganization of the hydrogen-bonding networks, possibly derived from unfolding of  $\alpha$ -helices in the linker region.

**4.4. Dynamics of the Conformational Change.** We fitted the TG signal in a whole time range based on the two state model (eq 5). Since  $D$  does not change so much by the photoadduct formation as shown by the LOV2 sample (Table 1),  $D$  of S390 of the LOV2-linker sample is assumed to be the same as that of D447. The best fitted parameters are summarized in Table 1. The remarkable agreement between the fitted and observed signals (Figure 3) indicates that the  $D$  change after the photoexcitation should be expressed by the two state model (Figure 6). The rate constant of the change determined from the fitting is  $(2 \text{ ms})^{-1}$ , indicating that the conformational change in the linker region related to the loss of  $\alpha$ -helicity takes place with the rate of  $(2 \text{ ms})^{-1}$ . The photoreaction process with the lifetime of 0.8–0.9  $\mu\text{s}$  (see section 4.2) associating with the adduct formation should trigger this conformational change. It is interesting to note the 3 orders of magnitude time delay from the triggering step to the global conformation change. The light-induced loss of  $\alpha$ -helicity monitored by the CD spectrum of oat Phot1 LOV2 occurs within the time resolution of the method, and the regeneration of  $\alpha$ -helicity occurs at the same rate as those in the visible region (45 s), indicating synchronous relaxation of protein and chromophore structures.<sup>18</sup> Since the time constant of the conformational change observed here (2 ms) is much faster than the regeneration step, this large delay may be characteristic with the adduct formation but not the relaxation processes.

Finally, we compare the results of this LOV2-linker sample with that of photoactive yellow protein (PYP), which is one of PAS domain family. In the PYP case, after the photoisomerization reaction of the chromophore (*p*-coumaric acid), the absorption spectrum changes to indicate the first intermediate species creation ( $pR_1$  species) followed by a spectrally silent process with 1  $\mu\text{s}$  ( $pR_2$ ) and subsequent absorption change by

the creation of another intermediate species (pB).<sup>32</sup> The time constant of the creation of the signaling species, which is presumably pB species, is around 200  $\mu$ s at room temperature, and this time constant is 5 orders of magnitude slower than that of the creation of the first intermediate species. The conformation of this species is dramatically changed from that of the ground (pG) state,<sup>33</sup> and  $D$  of the pB species is 1.2 times smaller than that of the pG species.<sup>34</sup> It is particularly interesting to note that the characteristics of pB (e.g., very long temporal delay for the conformation change after the triggering processes as well as the  $D$  change in the signaling state of PYP) are similar to those of the LOV2-linker sample studied here. The molecular origin of this large temporal delay as well as the  $D$  changes are to be investigated in future.

## Conclusion

Absorption spectroscopic studies have established the cyclic photochemical reactions in the LOV domains of phototropin. Only two photochemical intermediates, L660 (excited triplet state) and S390 (cysteinyl-flavine adduct) have been identified. This is characteristic with phototropin having a nonisomerizable chromophore, flavine, and quite a contrast to those of the other photoreceptors, such as rhodopsin or phytochrome, with the chromophore of retinal or tetrapyrrol, respectively, showing many photointermediates. Absorption spectra, however, reflect the electronic state around the chromophore and do not necessarily follow the molecular structure in the protein moiety. A Fourier transform infrared (FTIR) spectroscopic study<sup>35</sup> detected the secondary structural changes in the LOV2 domain

of *Adiantum* phytochrome3, and an NMR study found the changes in the interaction between the LOV2 domain and a part of linker region.<sup>17</sup> They cannot be seen by absorption spectroscopy.

In the present study, we monitored the photoreaction kinetics by the diffusion coefficient.  $D$  of the LOV2 sample decreases slightly by the adduct formation, which implies that the core shrinks slightly on adduct formation. After that change, no significant conformational change was observed. In the LOV2-linker, we found a novel distinct intermediate after the formation of S390 that appears with the rate constant of (2 ms)<sup>-1</sup>. This intermediate has a remarkably reduced diffusion constant that may come from the decrease of the  $\alpha$ -helicity in the linker region. Unfolding of J-helix has been reported, recently, to induce constitutive activation of kinase activity in the auto-phosphorylation, indicating the importance of  $\alpha$ -helicity in the linker region.<sup>36</sup> Furthermore, the LOV2 domain plays a crucial role in the photoregulation of kinase activity of substrate phosphorylation in *Arabidopsis* Phot2 (submitted). The present photointermediate with the reduced diffusion coefficient thus may reflect an important one involved in the photoregulation of the kinase activity.

Finally, kinetic study from a viewpoint of diffusion will supply useful information regarding the functions of a variety of important proteins in future.

**Acknowledgment.** This work is supported by the Grant-in-Aid (No. 13853002 and 15076204 to M.T. and 13139205 to S.T.) from the Ministry of Education, Science, Sports and Culture in Japan.

JA052523I

(32) Meyer, T. E.; van Grondelle, R.; Hellingwerf, K. J. *Biophys. J.* **1994**, *67*, 1691.

(33) Harigai, M.; Imamoto, Y.; Kamikubo, H.; Yamazaki, Y.; Kataoka, M. *Biochemistry* **2003**, *42*, 13893.

(34) Takeshita, K.; Imamoto, Y.; Kataoka, M.; Tokunaga, F.; Terazima, M. *Biochemistry* **2002**, *41*, 3037.

(35) Iwata, T.; Nozaki, D.; Tokutomi, S.; Kagawa, T.; Wada, M.; Kandori, M. *Biochemistry* **2003**, *42*, 8183.

(36) Harper, S. M.; Christie, J.; Gardner, K. H. *Biochemistry* **2004**, *43*, 16184.